water

MDPI

Article

Impact of Hill Fires on Dissolved Organic Matter in Watersheds of Karst Areas Based on Three-Dimensional Fluorescence-Parallel Factor Analysis

Kangming Shi [1], Huarong Zhao [1,2,3,*] and Zikang Ren [1]

[1] College of Environmental Science and Engineering, Guilin University of Technology, Guilin 541006, China; glutskm@163.com (K.S.); renzikang@glut.edu.cn (Z.R.)
[2] Collaborative Innovation Center for Water Pollution Control and Water Safety in Karst Area, Guilin University of Technology, Guilin 541006, China
[3] Guangxi Key Laboratory of Theory and Technology for Environmental Pollution Control, Guilin University of Technology, Guilin 541006, China
* Correspondence: zhaohuar@mail3.sysu.edu.cn

Abstract: Hill fires have the potential to influence dissolved organic matter (DOM) in water bodies, yet fewer studies have investigated the effects of hill fires on DOM within watersheds in karst areas. In this study, we employed the three-dimensional fluorescence-parallel factor analysis (EEM-PARAFAC) method to analyze the DOM fluorescence peaks, component compositions, fluorescence indices, and sources within the water body of the Yuanteng River sub-basin, which was impacted by the hill fire, serving as our primary research focus. The results indicate the presence of three primary fluorescent fractions in the water body of the Yuanteng River: C1, resembling humic acid (fulvic acid); C2, consisting of biopolymers and microbial by-products; and C3, containing proteins such as tyrosine and tryptophan. The Yuanteng River exhibited elevated levels of humus-like substances, diminished concentrations of protein-like substances, and demonstrated higher biogenic, freshness, and humification indices compared to unaffected water samples, reflecting the impact of the hill fire. Elevated levels of exogenous humic acid-like inputs into the waters of the Yuanteng River, along with exogenous inputs of DOM, were primarily influenced by stable, high-molecular-weight organic matter. Additionally, agricultural effluent, domestic sewage, and anthropogenic activities contributed to these inputs to a lesser degree. The impacts of endogenous inputs are mainly related to the restoration of ecosystems. The occurrence of hill fires has significantly influenced the composition of dissolved organic matter in the waters of the Yuanteng River. A comprehensive analysis of the impacts of hill fires on dissolved organic matter in water bodies can serve as a valuable reference for characterizing DOM in the water bodies of the Yuanteng River. Furthermore, it can inform strategies for environmental protection, facilitate the traceability of pollutants in water bodies, and contribute to environmental and ecological restoration efforts following hill fires in the region.

Keywords: hill fire; three-dimensional fluorescence spectroscopy; parallel factor analysis; fluorescence indices; dissolved organic matter

Citation: Shi, K.; Zhao, H.; Ren, Z. Impact of Hill Fires on Dissolved Organic Matter in Watersheds of Karst Areas Based on Three-Dimensional Fluorescence-Parallel Factor Analysis. *Water* **2024**, *16*, 1346. https://doi.org/10.3390/w16101346

Academic Editor: Mehrab Mehrvar

Received: 16 April 2024
Revised: 1 May 2024
Accepted: 6 May 2024
Published: 9 May 2024

1. Introduction

Dissolved organic matter (DOM) represents the predominant reservoir of organic matter found in all categories of natural waters [1,2]. Dissolved organic matter constitutes an exceedingly intricate organic amalgam capable of conducting biochemical processes within the water column. Its biological activity surpasses that of conventional organic matter, serving as the primary source of carbon and energy for microorganisms in ecosystems [3]. Sources of dissolved organic matter primarily encompass biological and terrestrial origins. Terrestrial sources entail the entry of organic matter into natural water bodies via processes such as the atmospheric cycle and the release of organic matter by ecosystems.

Biological sources entail the production of organic matter through the life processes of organisms within water bodies [4]. Research on the production, activities, and impacts of dissolved organic matter is crucial for understanding carbon cycling, biochemical transformations, ecological restoration, and ecosystem pollution management in areas affected by mountain fires.

Three-dimensional fluorescence spectroscopy serves as a prevalent method for characterizing dissolved organic matter in aqueous ecosystems, enabling the differentiation of fluorophores within the DOM. Fluorescence data about these fluorophores are presented in a three-dimensional excitation matrix known as the Excitation–Emission Matrix (EEM), where excitation and emission wavelengths serve as indicators of fluorescence intensity [5]. The intensity of fluorescence is indicated by excitation and emission wavelengths. Due to the potential superposition of peaks during the detection and recognition of fluorophores, leading to incomplete or unrecognized EEM spectra, the obtained EEM spectra can be effectively analyzed by integrating the parallel factor analysis (PARAFAC) method. This approach allows for the identification and differentiation of the number of fluorophores, fluorescence intensity, and other pertinent information [6]. Three-dimensional fluorescence spectroscopy is extensively employed in dissolved organic matter research due to its high sensitivity, rapid and precise identification, and minimal sample volume requirements [7]. Zhi et al. [4] investigated dissolved organic matter in artificial wetlands, demonstrating that the EEM-PARAFAC technique serves as an effective approach for examining the extent of DOM humification in aquatic environments. Kellerman et al. [8] conducted detection and analysis of dissolved organic matter in Swedish lakes, revealing that aromatic compounds exhibit preferential decomposition under environmental factors governing DOM decomposition, while aliphatic and nitrogenous compounds manifest in diverse forms within the water column. Wen et al. [9] investigated effluent from a wastewater treatment plant using three-dimensional fluorescence spectroscopy and demonstrated that the humic index can serve as a straightforward proxy for representing certain chemical components. Shang et al. [10] analyzed the source and composition of DOM in numerous humus- and protein-rich lakes in China, demonstrating that anthropogenic activities have heightened the sourcing, transformation, and degradation of DOM. Tetsuro Kikuchi et al. [11] examined the relationship between DOM and trace metals in both natural and sewage water, revealing that dissolved copper and iron concentrations were influenced by DOM concentration and the presence of aromatic DOM. Chen et al. [12] investigated the composition of dissolved organic matter in surface waters across various river reaches, elucidating the influence of UV light and hydrological conditions on terrestrial humus content. Moreover, they revealed that DOM exhibits distinct photoresponsive characteristics. Wang et al. [13] explored the transformation of dissolved organic matter along the Yangtze River in China across varying hydrological conditions, establishing a correlation between the chemical composition of DOM and optical conditions. Their findings underscored the impacts of photoresponse and soil erosion on DOM content and composition. The aforementioned studies demonstrate that the EEM-PARAFAC technique is widely employed as a method and technique for resolving the compositional components, sources, and quantitative analysis of DOM.

Hill fires can lead to contamination of surface waters within the burned area with dissolved organic matter, and the extent of this contamination varies depending on the size of the hill fires. The composition of dissolved organic matter and organic compounds is intricate. Following hill fires, there is a notable increase in aromatic and humic DOM within water bodies. Moreover, the contamination of soil and surface water is influenced by a combination of ecological factors, rainfall, and surface runoff [14]. Youhei Yamashita et al. [15] investigated carbonized sediments generated after a hill fire, demonstrating that the transfer of carbonized sediments correlates with high-molecular-weight aromatic DOM, and the conversion relationship is intricate. David Olefeldt et al. [16] investigated the impacts of mountain fires on dissolved organic matter production and the composition of forested soils. Their findings demonstrated that mountain fires have the potential to modify DOM turnover in soils and influence the interplay between terrestrial and aquatic carbon cycling. Vergnoux et al. [17] investigated the impact of hill fires on soil organic matter and subsequent soil recovery. Their research revealed that hill fires directly influenced soil humus content and that humus aromaticity exhibited prolonged increases following hill fires. Dymov et al. [18] investigated the organic matter of surface soils post-hill fires, revealing differences in aromaticity and phenyl polycarboxylic acidity compared to the initial soil. Additionally, soil acidification resulted in a reduction in the surface area of the organic layer. Li et al. [19] examined the impacts of mountain fires on the distribution of soil carbon and other nutrients in the mountainous regions of northern Daxinganling. Their findings revealed that the soil environment exhibited a weakly acidic nature following the fires. Additionally, the carbon and nitrogen contents of soils in the burned areas experienced substantial reductions, persisting below normal levels for an extended period. Bladon et al. [20] conducted an analysis of nitrogen levels in water bodies within the burned area of the hill fire and investigated the initial restoration of water quality post-fire. Their findings indicated that water bodies affected by the hill fire exhibited elevated nitrogen levels, particularly during periods of increased water availability. Hill fires are among the most common disasters globally, resulting in the burning of vegetation and damage to soil, thereby impacting the stability of ecosystems. Pollution from dissolved organic matter has the potential to adversely affect both surface and groundwater, thereby compromising the health of aquatic ecosystems. Currently, there is a dearth of research on the impact of hill fires in the mountainous regions of Guangxi on dissolved organic matter within local water bodies. Hence, investigating the influence of hill fires on DOM in water bodies holds significant importance.

In recent years, the investigation of dissolved organic matter in water bodies using three-dimensional fluorescence spectroscopy and parallel factor analysis has emerged as a key research focus. The spectral resolution of dissolved organic matter can effectively characterize the DOM source, composition, spatial and temporal distribution, and chemical properties. This study focused on the Yuanteng River, situated in the vicinity of the mountain fire in Rongjiang Town, Xing'an County, Guangxi, serving as the primary study area. Various analytical techniques including three-dimensional fluorescence spectroscopy and parallel factor analysis methods were employed to investigate the composition and sources of dissolved organic matter within the Yuanteng River water body; examine the sources and impacts of water pollution caused by dissolved organic matter resulting from hill fires; offer robust evidence and a scientific foundation to support the investigation of dissolved organic matter characterization, environmental protection, water pollutant tracing, and ecological restoration in the Yuanteng River watershed; furnish theoretical underpinnings to aid local governments in assessing ecosystem resilience, formulating strategies for water quality pollution remediation, devising ecological restoration plans, and implementing forest management measures; and mitigate the adverse environmental effects of fires, raise awareness among villagers about fire hazards, and advocate for sustainable management and utilization of natural resources.

2. Materials and Methods

2.1. Overview of Study Area

The study area is situated in Rongjiang Town, within Xing'an County, Guilin City, Guangxi, China, spanning from 110°14′ to 110°56′ E longitude and 25°17′ to 25°55′ N latitude. The geomorphology of the study area is karstic. Xing'an County covers a total land area of 2348 km^2, with an east–west horizontal distance of 70 km and a north–south vertical distance of 68 km. It experiences a subtropical humid monsoon climate characterized by abundant rainfall and sunshine, with an average annual temperature of 18.2 °C, an average annual relative humidity of 79%, annual sunshine hours ranging from 1300 to 1800 h, and an average annual rainfall of approximately 1942.9 mm. Xing'an County serves as the origin of both the Li River and the Xiang River. Additionally, the Lingqu River flows southwestward into the Rong River, where it converges with the Li River. Xing'an County exhibits a diverse and intricate topography, featuring mountainous terrain in the northwest and southeast regions. The landscape is characterized by overlapping mountains, ravines, and numerous streams. To the northwest is the Echungling Mountain System, which gradually slopes to the southwest. To the southeast is the oceanic mountain system of the Dupont Ridge, which slopes gradually to the northeast. The forest vegetation in Xing'an County primarily comprises deciduous broad-leaved forests and evergreen broad-leaved forests. It includes high-altitude species like green oak, alpine rhododendron, wild star anise, and South China hemlock, as well as broad-leaved dwarf forests such as Houpao and Rosewood. The low-altitude vegetation comprises species such as fir, horsetail pine, moso bamboo, oleander, oil tea, white fruit, citrus, and others. Rongjiang Town boasts 3789 hectares of arable land, encompassing 3122 hectares dedicated to paddy fields and an additional 35,466.6 hectares designated for forested purposes. The primary mineral resources present in the area encompass hematite, lead–zinc ore, and alluvial gold deposits. On 28 January 2023, a hillside conflagration erupted in Rongjiang Town, situated within Xing'an County, Guilin City. This inferno spanned a fire line measuring approximately 1.6 km in length, scorching an expanse exceeding 240 acres. The blaze left in its wake a substantial accumulation of charred vegetation, resembling blackened charcoal, strewn across the earth's surface. The dispersion of yellow smoke and ash from the hillside conflagrations had a widespread impact on numerous villages and urban areas located downhill. Additionally, it led to the contamination of woodland catchments and mountain streams. Among these areas, the Yuanteng River, situated in Huangjia Village within the study zone, bore the brunt of the hill fires, experiencing the most severe consequences.

2.2. Sample Acquisition

In July 2023, samples necessary for the study were collected. A total of twelve sampling sites were strategically established along the continuum from upstream to downstream, guided by the spatial distribution of streams within the study area. The sampling sites are depicted in Figure 1. Sites 1–9 were selected along the Yuanteng River, the area most impacted by the hill fires. Sites 10–11 were situated along the Li River, while site 12 was positioned along the Ku River.

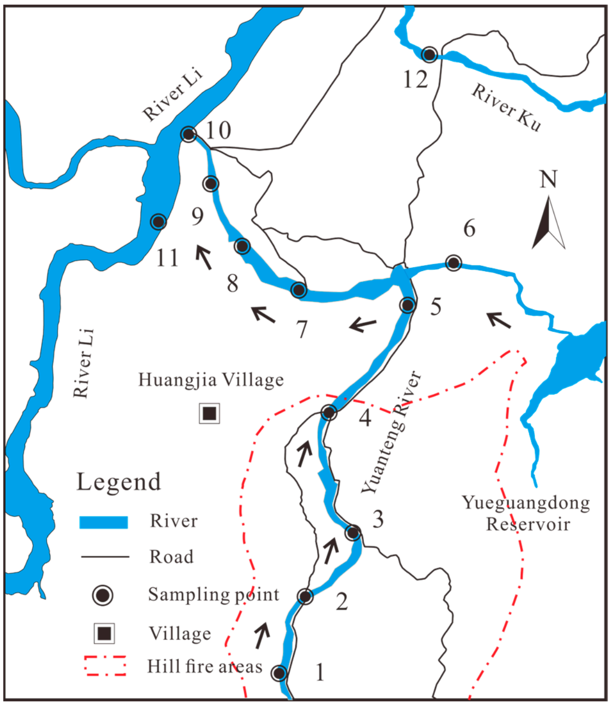

Figure 1. Overview of the study area and sampling schematic.

The sampling points were precisely identified utilizing GPS technology. Subsequently, the sampling bottles underwent thorough cleaning with ultrapure water followed by natural air drying. Subsequently, 2 L of surface water were collected from each sampling point and dispensed into light-proof glass bottles, which were then sequentially numbered. Upon transportation back to the laboratory, the samples underwent filtration using a 0.45 μm membrane and were subsequently stored under refrigeration at 4 °C. All samples collected were tested and analyzed within one week.

2.3. Sample Analysis Methods

2.3.1. Three-Dimensional Fluorescence Spectrometry

Three-dimensional fluorescence spectroscopy measurements were conducted utilizing the HORIBA Aqualog-Water Environment Research Analyzer. A 10 mm four-way quartz cuvette was employed to establish the excitation wavelength (Ex) range from 240 to 500 nm with an excitation increment of 3 nm, the emission wavelength (Em) range from 240 to 500 nm with a step size of 5 nm, and an integration time of 1 s. Milli-Q ultrapure water served as the blank for Raman scattering removal, and the scanning spectra were automatically corrected by the instrument.

2.3.2. Parallel Factor Analysis and Spectral Index Calculation

Three-dimensional fluorescence spectra (EEMs) underwent data preprocessing in Excel, with blanks subtracted to mitigate the effects of Raman scattering, and subsequently analyzed for parallel factor analysis utilizing the DOMFluor toolbox, as follows: (1) Importing data for the removal of primary and secondary Rayleigh scattering. (2) Preliminary data analysis involved the identification and removal of outliers. (3) Validation of residual values followed by the determination of group scores. (4) The halves were split and analyzed for anomalies, followed by consistency tests. (5) Randomized initial analytical validation of experimental results obtained from split-half analysis. (6) Plotting Component Maps and Component Load Maps. (7) Outputting the fluorescence data of each component along with the maximum fluorescence intensity. (8) Calculation of the fluorescence characterization index. The main fluorescence characterization indices calculated included the freshness index (FRI), humification index (HIX), biological index (BIX), fluorescence index (FI), and other related indices. The formula is presented as follows [21–23]:

$$FRI = \frac{F(Em = 310\ \text{nm}, Em = 380\ \text{nm})}{F(\,Ex = 310\ \text{nm}, Em = 420\ \sim 435\ \text{nm})} \tag{1}$$

$$HIX = \frac{F(\,Ex = 255\ \text{nm}, Em = 435\ \sim 480\ \text{nm})}{F(\,Ex = 255\ \text{nm}, Em = 300\ \sim 345\ \text{nm})} \tag{2}$$

$$BIX = \frac{F(Ex = 310\ \text{nm}, Em = 380\ \text{nm})}{F(Ex = 310\ \text{nm}, Em = 430\ \text{nm})} \tag{3}$$

$$FI = \frac{F(Ex = 370\ \text{nm}, Em = 470\ \text{nm})}{F(Ex = 370\ \text{nm}, Em = 520\ \text{nm})} \tag{4}$$

2.3.3. Data Processing Analysis and Statistics

Excel software was utilized for data processing. Parallel factor analysis, component plotting, correlation index calculation, and EEM plotting were conducted in MATLAB 2015b software using the DOMFluor toolbox. Correlation data analysis and statistics were carried out using SPSS20 software, and plots were generated using Origin2021 student edition software.

3. Results and Analysis

3.1. DOM Fluorescence Peak Characteristics

The three-dimensional fluorescence spectra of the Yuanteng River water body can be computed through index calculation and analyzed based on the corresponding components, with the main types of fluorescence peaks depicted in Table 1. Figure 2 illustrates selected three-dimensional fluorescence spectra of major fluorescence peaks in both the plan view and surface view. Specifically, Figure 2a,b depict UV-like humic substances, Figure 2c,d represent visible humic substances, Figure 2e,f display tyrosine-like proteins, and Figure 2g,h present tryptophan-like proteins. The water of the Yuanteng River flows from mountainous water bodies at sampling points 1 to 3, passes through water bodies of farmers raising poultry at sampling point 4, continues through farmland water bodies at sampling point 5, and then converges with water bodies from the Yueguangdong Reservoir at sampling point 6. Subsequently, it flows through farmland water bodies at sampling points 7 to 9, traverses villages, and ultimately merges with the water bodies of the Li River at sampling points 10 and 11. Sampling site 12 represents a water body of the Ku River. Sampling points 1 to 9 denote water bodies of the Yuanteng River, which were impacted by the hill fire, while sampling points 10 to 12 encompass water bodies of both the Li River and the Ku River, unaffected by the hill fire.

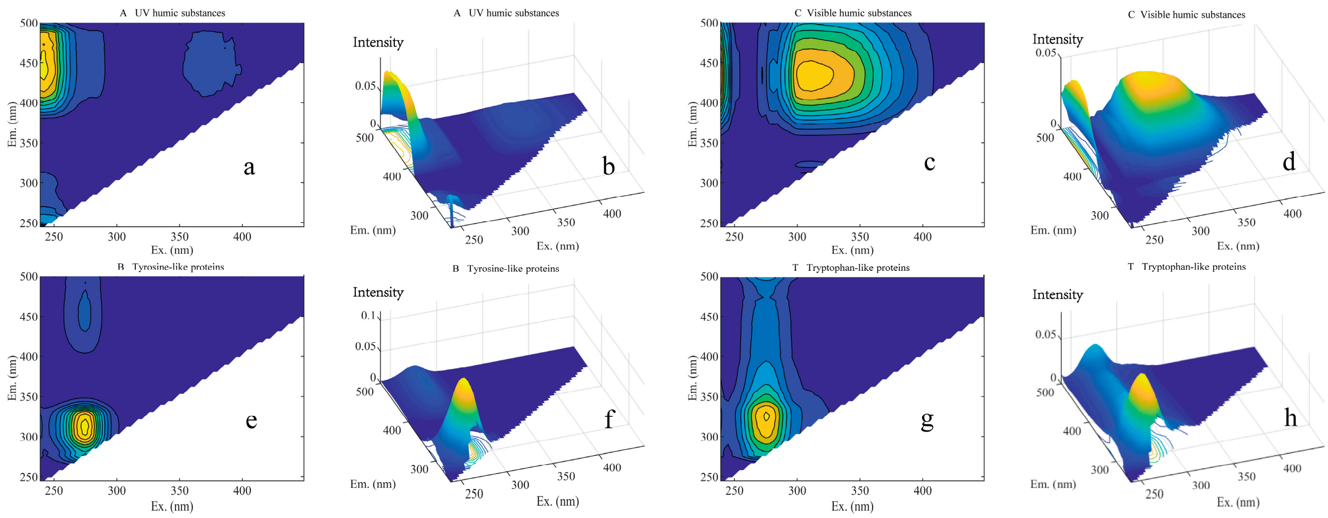

Figure 2. Three-dimensional fluorescence spectra of major fluorescence peaks (UV humic sub-stances (**a**,**b**), visible humic substances (**c**,**d**), tyrosine-like proteins (**e**,**f**), tryptophan-like proteins (**g**,**h**)).

The three-dimensional fluorescence characteristic peak A, representing UV-like humic acid, is a prevalent feature in surface water bodies, while peak C, corresponding to the visible region of humic acid, is typically employed for analyzing land-based sources of humic acid. The B and T peaks, representing tyrosine and tryptophan of the protein group, primarily arise from biological enzymes released during bacterial decomposition, as well as from amino acids and proteins derived from aquatic plants, proteins present in the remnants of aquatic organisms, and anthropogenic activities [24].

Peaks A and C were predominantly observed in the mountainous waters of the Yuanteng River, exhibiting a general upward trend with the flow direction, while peak T was absent in the hill waters. Following high temperatures, alterations occur in the surface soil microbial community, resulting in affected microbial life activities and diminished capacity for the decomposition of dissolved organic matter. Consequently, a significant portion of molecular organic matter with a novel structure that is less prone to dissolution is formed. Vegetation affected by hill fires, along with vegetation that has not completely combusted, undergoes gradual decay due to the effects of rainfall and microbial action in deeper soil layers. This process results in the formation of stable small-molecule organic matter through the decomposition of lignin and the oxidation of aromatic and aldehyde groups during soil release. The transportation of newly structured molecular organic matter and stabilized small-molecule organic matter, as they pass through the surface and sink into waters affected by mountain fires, leads to an elevation in the fluorescence intensity of humus-like peaks and the content of novel organic matter.

Peaks A, C, and B were detected in the water of poultry farms along the Yuanteng River. Peak A exhibits its distinctive fluorescence feature because the primary source of the water body is predominantly mountainous. The notable fluorescence of peak B, on the other hand, stems from the presence of poultry urine, feces, and feed residues in the water column, all of which contain substantial amounts of protein. Enzymes produced through microbial life activities and bacterial decomposition in the water body, along with aromatic ring amino acids released from biological remains, combine with certain molecules to generate new organic matter. This process leads to an increase in the organic matter content within the water body of the poultry farm. Additionally, proteins undergo hydrolysis under the action of proteolytic enzymes, resulting in the formation of amino acids, consequently leading to a notable enhancement of peaks associated with protein components [25–27].

Peaks A, B, C, and T were observed in the farmland water of the Yuanteng River, with the fluorescence intensity of peaks C and T being weaker compared to peak A. Peaks A and C exhibited similar characteristics as observed in the mountainous waters, with a gradual increase in fluorescence intensity observed with water flow. On one hand, the extended decay period and advanced degree of decay of biological debris in farmers' aquaculture waters result in the emergence of humic acid-like, tryptophan-like, and protein-like fluorophores due to microbial and photodegradation processes [28]. On the other hand, due to farmland fertilization, a certain amount of nitrogen fertilizer leads to increased microbial activity in farmland soils, which improves the degradation of dissolved organic matter, accelerates protein decomposition, increases the accumulation of lignin and cellulose, and increases the level of aromatization and humification of organic matter, which leads to an increase in the intensity of humic acid-like fluorophores within this water [29].

Peak B and peak A are evident in the water column of Yueguangdong Reservoir. Reservoir water has accumulated over a long period, the water is highly humified, and the water has a low protein content. Waters affected by hill fires converged at sampling sites 5 and 6 before flowing through the farmland, leading to a decrease in protein-like peak fluorophores and a notable increase in humic acid-like fluorophores. The heightened significance of peak A and C fluorophores in the water bodies of the Li River at sampling sites 10 and 11, compared to those in the mountainous water bodies of the Yuanteng River, and their comparable significance to those in the farmland water bodies of the Yuanteng River, may be attributed to the location of the sampling sites at the confluence of tributary streams and the Li River in the study area. The water body of the Ku River at sampling point 12 exhibited the highest fluorescence intensity of peak B, followed by peak T, and the lowest fluorescence intensity of peaks A and C.

The protein-like fluorescence peaks exhibited significantly higher intensity, while the humus-like peaks displayed notably lower intensity in the water bodies at sampling sites 10 to 12 compared to those in the Yuanteng River waters. This implies that the burning of hill fires led to the consumption of a significant amount of proteins from the vegetation. As a consequence, the protein-like peaks observed in the water after the fires had a much lower intensity compared to the typical levels in the region. The accelerated decay of burned vegetation led to the emergence of significantly higher humus-like peaks compared to those observed in normal waters.

Table 1. The main types of fluorescence peaks in the water bodies of the study area.

Main Peaks	Sample ID	Fluorescence Peak Type
A	1~12	UV humus [5,21]
B	1,4~8,10~12	Protein-like (tyrosine-like) [5,21]
C	1,2,4,6~12	Visible humus [30,31]
T	6~8,10,12	Protein-like (tryptophan-like) [30]

3.2. Analysis of Water Column Components

Analysis of the three-dimensional fluorescence spectra was conducted employing the EEM-PARAFAC method. Water samples from sampling points 1 to 9 of the Yuanteng River, impacted by the hill fire, were grouped into one category, while water samples from sampling points 10 to 12 of the Li River and the Ku River, unaffected by the hill fire, were grouped into another category. Three fractions—humus-like fulvic acid, protein-like, and protein-like (microbial by-products and biopolymers)—were identified in the water body of the Yuanteng River impacted by the hill fire. Two fractions of humus-like fulvic acid and two fractions of protein-like, amounting to a total of five fluorescent fractions, were identified in the water unaffected by the hill fire. Table 2 presents the characterization of five fluorescence fractions in the dissolved organic matter of water bodies in the study area. Additionally, Figure 3 displays the five fluorescence component loading diagrams analyzed by the EEM-PARAFAC model for the water bodies in the study area. In Figure 3, A represents the C1 component diagram, B represents the C1 component loading diagram, C represents the C2 component diagram, D represents the C2 component loading diagram, E represents the C3 component diagram, F represents the C3 component loading diagram, G represents the C4 component diagram, H represents the C4 component loading diagram, I represents the C5 component diagram, and J denotes the C5 component loading diagram. It is worth noting that C1 to C3 represent the water body components of the Yuanteng River, while C4 to C5 represent normal water bodies. All analyzed components underwent data comparison with the online open fluorescence database (https://openfluor.lablicate.com (accessed on 3 July 2023)), demonstrating a similarity of more than 95% in component fluorescence data.

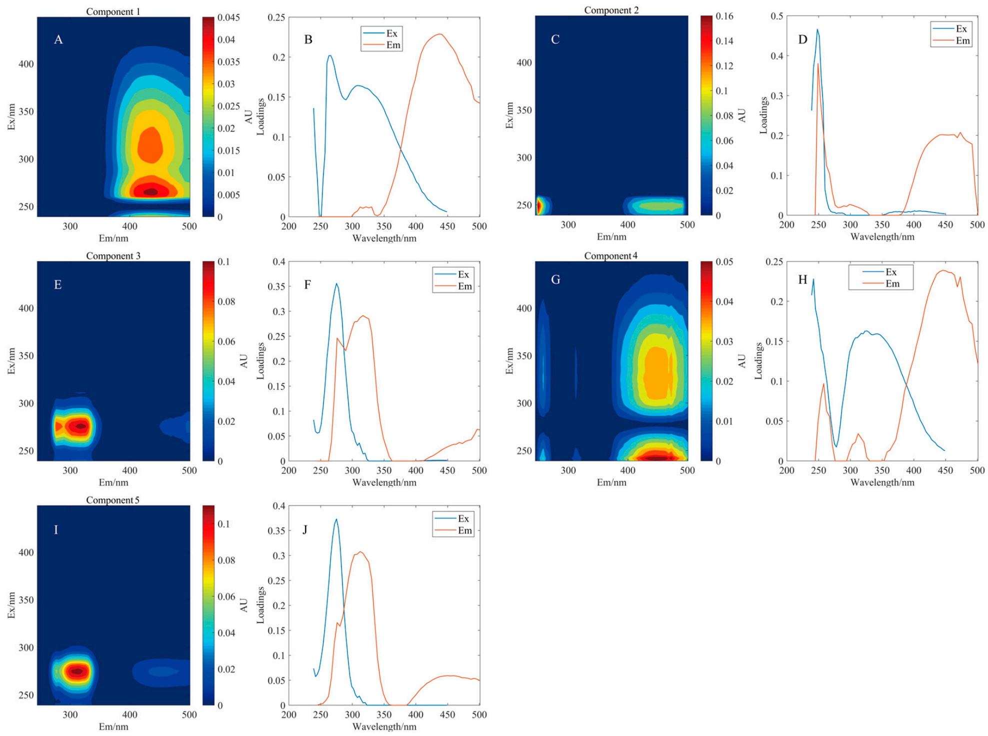

Figure 3. Load map of the five fluorescence components analyzed by the EEM-PARAFAC model ((**A**) indicates C1 component diagram, (**B**) indicates C1 component load diagram, (**C**) indicates C2 component diagram, (**D**) indicates C2 component load diagram, (**E**) indicates C3 component diagram, (**F**) indicates C3 component load diagram, (**G**) indicates C4 component diagram, (**H**) indicates C4 component load diagram, (**I**) indicates C5 component diagram, (**J**) indicates C5 component load diagram).

Components C1 and C4 are classified as humic-like fulvic acids, characterized by two excitation peaks and one emission peak. The short-wave excitation peaks, characteristic of traditional peaks of peak A, are situated in the position of short-wave humic-like substances, while the long-wave excitation peaks, characteristic of traditional peaks of peak C, correspond to fulvic-like substances. Furthermore, UV fulvic-like and visible fulvic-like substances are associated with carbonyl and hydroxyl groups. The content of visible fulvic acid is lower compared to UV fulvic acid. The primary source of humus-like substances in flowing water is exogenous. UV fulvic acid is generated from high aromatic compounds with high molecular weight and stability in organic matter, characterized by a complex structure that is resistant to photodegradation and biodegradation [32]. Humic acid-like levels are lower in normal waters compared to those in the Yuanteng River waters. The redshift observed in the peak of component C1 may be attributed to the elevated concentration of aromatic compounds present in the water column [33]. Component C2 exhibits one excitation peak and two emission peaks. The short-wave emission peaks are associated with microbial byproducts and biopolymers, while the long-wave emission peaks correspond to humic-like fulvic acid peaks observed in the conventional A peaks [5,27] Both C3 and C5 are categorized as traditional protein-like peaks, with the package class comprising tyrosine- and tryptophan-like proteins. The fluorescence intensity of the protein-like fractions exceeded that of the humic-like fractions. Tyrosine-like proteins are linked to aromatic ring amino acids, while tryptophan-like proteins originate from amino acids generated during the decomposition of terrestrial plants and organic matter in the soil [22]. The protein-like fluorescence intensity of component C3 was lower than that of component C5 in normal waters, possibly due to the tyrosine-like proteins originating from microbial and terrestrial sources of influence. During the summer sampling season, elevated water temperatures facilitated microbial activity in the water column, leading to the hydrolysis of proteins into amino acids by microbial action and subsequently increasing the concentration of protein-like substances. The hill fires resulted in the burning of the majority of surface terrestrial plants, which primarily consisted of plants with low protein content. The hill fires left most of the surface terrestrial plants burned, originating from the low protein content of terrestrial plants, with a small fraction originating from inadequately burned terrestrial plants, and the majority from terrestrial sources of microbial impacts from agricultural runoff and domestic wastewater along the way, food residues, and organic matter from a portion of the deeper soils. Components C1 to C3 serve as the primary representative components of the water body of the Yuanteng River, in contrast to components C4 to C5 of the water body unaffected by the hill fire. The fluorescence intensity of the humic-like fulvic acid component is substantial, whereas the fluorescence intensity of the protein-like component is relatively small. Furthermore, the fluorescence intensity of protein-like fluorescence generally exceeds that of humic-like fluorescence. Water bodies impacted by hill fires also exhibit the presence of microbial by-products and biopolymer fluorophores.

Table 2. Characterization of DOM fluorescence fractions in water bodies in the study area.

Components	Typology	Study Area		Reference	
		Ex	Em	Ex	Em
C1	Humus-like fulvic acid	265/296–332	422–445	230–260	380–480 [34]
				300–380	400–480 [35]
C2	Humus-like fulvic acid, microbial by-products, biopolymers	250	249/422–480	250–300	250–390 [5]
				230–260	380–480 [34]
C3	pepsin-like protein	275	290–320	270–280	300–320 [36]
C4	Humic acid-like fulvic acid	242/308–353	436–473	230–260	380–480 [35]
				300–380	400–480 [34]
C5	pepsin-like protein	275	305–320	270–280	300–320 [36]

3.3. Fluorescence Characterization Parameters

The three-dimensional fluorescence characterization index typically encompasses the fluorescence index (FI), freshness index (FRI), biogenic index (BIX), and humification index (HIX). Figure 4 depicts the fluorescence parameters of the water bodies in the study area. Figure 4 depicts the fluorescence parameters, with (a) representing the fluorescence index, (b) representing the biogenic index, (c) representing the freshness index, and (d) representing the humification index.

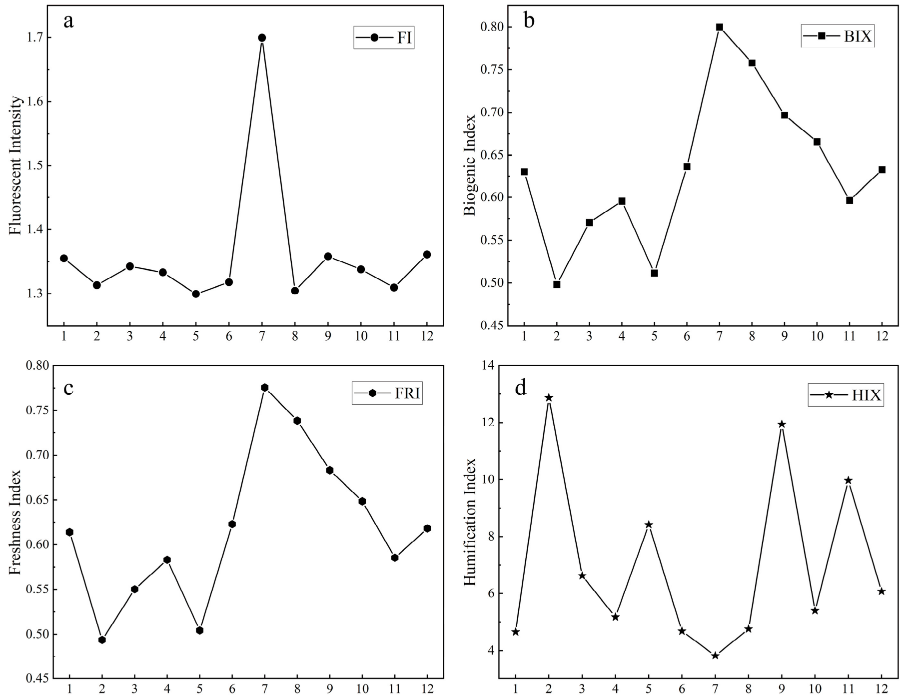

Figure 4. The plot of 4 fluorescence parameters of water bodies in the study area ((**a**) fluorescence index, (**b**) biogenicity index, (**c**) freshness index, (**d**) humification index).

The fluorescence index serves as a critical indicator for identifying the source of dissolved organic matter. When FI < 1.4, it signifies that terrestrial inputs dominate the source of DOM, while FI > 1.9 indicates that autochthonous sources predominate. A range of FI = 1.4~1.9 suggests a mixture of both terrestrial and autochthonous inputs for the source of DOM [33]. The FI index at the sampling sites ranged from 1.3 to 1.7, indicating strong autogenous source inputs to the dissolved organic matter at sampling site 7, and a combination of terrestrial and autogenous source inputs to the DOM at sampling site 12.

The freshness index FRI represents the proportion of de novo DOM, with higher values indicating a greater de novo DOM content. The FRI values at the sampling points ranged from 0.49 to 0.77, suggesting a higher proportion of nascent DOM at sampling point 7 and lower nascent DOM content at the other sampling points.

The biogenicity index BIX is employed to assess autochthonous dissolved organic matter [37]. A BIX value greater than 1.0 indicates that DOM is primarily autochthonous, while BIX values ranging from 0.8 to 1.0 suggest a higher proportion of nascent DOM in the samples. In the range of 0.6 to 0.8, BIX signifies contributions from both autochthonous and terrestrial sources, whereas BIX values below 0.6 indicate that DOM is predominantly terrestrial [21,38]. The BIX values at the sampling sites ranged from 0.5 to 0.8, indicating the presence of both autochthonous and terrestrial inputs in the dissolved organic matter sources. This finding aligns with the performance results of the FRI index.

The humification index (HIX) is employed to assess the degree of DOM humification. A HIX value greater than 6.0 indicates that DOM is strongly humified and primarily influenced by terrestrial inputs, while HIX values ranging from 4.0 to 6.0 suggest weak humification with strong contributions from autochthonous sources. A HIX value below 4.0 indicates weak humification predominantly influenced by autochthonous sources [21,39]. HIX values between 4.0 and 6.0 for sampling sites 1, 4, 8, and 10 indicate weak humification and strong autochthonous sources. HIX values exceeding 6.0 at sampling points 2, 3, 5, 6, 9, 11, and 2 suggest strong humification characterized by predominantly terrestrial inputs.

4. Discussions

Samples were analyzed five months following the occurrence of the hill fire. The study area experienced relatively dry conditions with low rainfall during the interval between the hill fire and the time of sampling. Environmental factors such as rainfall, temperature, and sunlight exert influence on dissolved organic matter in the Yuanteng River. Consequently, these conditions would likely lead to lower levels of DOM originating from the Yuanteng River compared to those from the Yuanteng River at the onset of the hill fire. Nonetheless, the effects of the hill fire on the Source Yuanteng River DOM are markedly more pronounced in contrast to water bodies unaffected by the hill fire.

4.1. DOM Source Impact

The FI index was employed to discern the various sources of dissolved organic matter, revealing that within the study area, DOM present in the water bodies of the Yuanteng River, influenced by hill fires, exhibited contributions from both terrestrial sources and microbial processes. Apart from sampling site 7, the other sampling sites impacted by the hill fire showcased characteristic humus-dissolved organic matter traits originating from terrestrial sources. The elevated microbial activity observed at sampling site 7 can be attributed to anthropogenic influences, particularly the impact of domestic wastewater and agricultural runoff, indicating a prevalence of autochthonous sources at this site. Consequently, the FI values are particularly responsive in water bodies characterized by terrestrial inputs.

The BIX index, applied to the water bodies within the study area, delineates the presence of both endogenous and exogenous inputs of biogenic dissolved organic matter, serving as an indicator of the proportion of de novo DOM contribution, wherein lower values signify a diminished presence of endogenous DOM. The diminished biogenic index observed in the Yuanteng River's water body stems from the generation of novel organic compounds resistant to degradation, a consequence of mountain fires that attenuate the biodegradation potential within the aquatic environment, while the predominant organic matter originates predominantly from terrestrial sources. A decreased BIX index signifies heightened anthropogenic influence, while the elevated BIX index observed in the farmland water body of the Yuanteng River, particularly at sampling site 7, likely stems from anthropogenic pollution, augmented microbial and zooplankton activity, and amplified bacterial presence, aligning with the trends delineated by the FRI index.

The HIX index analysis conducted on the Yuanteng River's waters reveals a predominant contribution of humus-like dissolved organic matter. The ecological and chemical characteristics of surface soils may have undergone modifications after the hill fires, with the accumulation of burned soils, coke, and partially combusted terrestrial vegetation potentially giving rise to stable, high-molecular-weight aromatic dissolved organic matter through percolation. This material could have been introduced into the river and transformed into humus-like DOM under the influence of UV radiation, thereby augmenting the endogenous influx of humus into the waters of the Yuanteng River, which was impacted by the hill fires [16].

The average HIX index of the pristine water bodies was lower than that of the Yuanteng River, accompanied by a higher humic acid-like fluorescence intensity observed in the 3D fluorescence spectra of the Yuanteng River's water body compared to the normal water body. These findings suggest that the influence of the hill fire has resulted in an augmentation of humus-like dissolved organic matter in the Yuanteng River's water body. Furthermore, mountainous water bodies and reservoirs affected by the hill fire exhibit a substantial presence of highly aromatic DOM, continuously transported downstream via seepage flow. The elevated HIX index recorded at sampling point 11 within the pristine water body could be attributed to its proximity to the outfall of farmland in Huangjia Village. It is plausible that the infiltration of humus-like dissolved organic matter from farmland wastewater into the Yuanteng River's water body has contributed to the heightened humus index observed at sampling point 11.

The fluorescence intensity of protein-like DOM in the waters of the Yuanteng River was less than that of normal waters. The soil microbial community undergoes alteration in response to mountain fires, resulting in diminished organic matter input and reduced microbial degradation capacity within water bodies. Consequently, there is a decline in the content of endogenous protein input in mountain water bodies. As water body flow progresses, exogenous protein inputs dominate, potentially impeding organic matter decomposition by microbial action, thus fostering the emergence of a novel structural configuration. Protein-like dissolved organic matter inputs in typical water bodies originate partly from soil organic matter and partly from sources including domestic wastewater from villagers, poultry feces, and food residues.

The water bodies of the Yuanteng River, affected by the hill fire, exhibit a blend of exogenous and endogenous inputs influencing the dynamics of dissolved organic matter sources. The impact of the hill fires manifests in elevated humic-like DOM content and heightened fluorescence intensity compared to protein-like DOM. On the one hand, the fluorescent-like humus originating from burned terrestrial plants and terrestrial DOM in surface soils enter the water body and are further decomposed, and on the other hand, the readily decomposable nutrients, such as nitrogen, phosphorus, and amino acids, contained in domestic wastes and agricultural wastewater, which are decomposed by microorganisms to produce protein-like fluorescent substances and nascent microbial byproducts and biopolymers that do not readily decompose.

4.2. Correlation Analysis

Figure 5 displays the correlation analysis between dissolved organic matter fractions and fluorescence indices of water bodies in the Yuanteng River impacted by the hill fire. The C1 humus component, enriched with C2 humus and microbial by-products, exhibits a notable correlation with biopolymer components. Additionally, its long-wave emission peaks, characteristic of humic fulvic acid, share a common origin, originating from the same fluorophore and possessing typical terrestrial characteristics. The generation of microbial by-products and biopolymer-dissolved organic matter within the C2 fraction may be linked to the formation of shortwave-like humic substances characterized by photolysis, high molecular weights, and complex structures. Both the C1 and C2 fractions exhibited significant negative correlations with the C3 protein-like fractions, indicating variability in the composition of their dissolved organic matter sources, comprising distinct origins for humus-like and protein-like fractions. The decay value index of the HIX showed a significant positive correlation with the C1 fraction and a significant negative correlation with the C3 fraction. This suggests that decay magnitude is positively associated with the fluorescence intensity of humic substances and inversely related to the fluorescence intensity of tyrosine, consistent with the findings of the source impact analysis. The biogenic index and the freshness index exhibited a significant positive correlation, indicating consistent variation in the source and composition of dissolved organic matter in the water column.

4.3. Source Analysis of DOM Composition

Figure 6 illustrates the presence of both endogenous and exogenous contributions to the sources of dissolved organic matter in the Yuanteng River, particularly under the influence of mountain fires. Four primary pathways contribute to the composition of dissolved organic matter in the water body of the Yuanteng River under exogenous effects: the rainfall pathway, the farmland runoff pathway, the pathway of domestic and aquaculture wastewater, and the pathway of photochemical reactions. Humus-like and protein-like dissolved organic matter from surface soils is transported to the waters of the

Yuanteng River via surface runoff during rainfall events along the rainfall pathway. Within the trajectory of farmland decline, humus-like and protein-like dissolved organic matter originating from farmlands has been observed to permeate into the aquatic environment of the Yuanteng River through processes such as irrigation, rainfall, and various other pathways. Both domestic wastewater and aquaculture effluents harbor substantial quantities of organic matter and bacteria, primarily comprising protein-like substances constituting the dominant dissolved organic matter fraction, subsequently undergoing treatment processes before discharge into the aquatic ecosystem of the Yuanteng River. Within the framework of the photoreaction pathway, black charcoal generated from mountain fires infiltrates the aquatic environment of the Yuanteng River, engaging in interactions with DOM_1 (dissolved organic matter native to the Yuanteng River), resulting in the production of DOM_2 (humus-like substance), biopolymers, and microbial by-products through UV-mediated reactions, subsequently emitting CO_2.

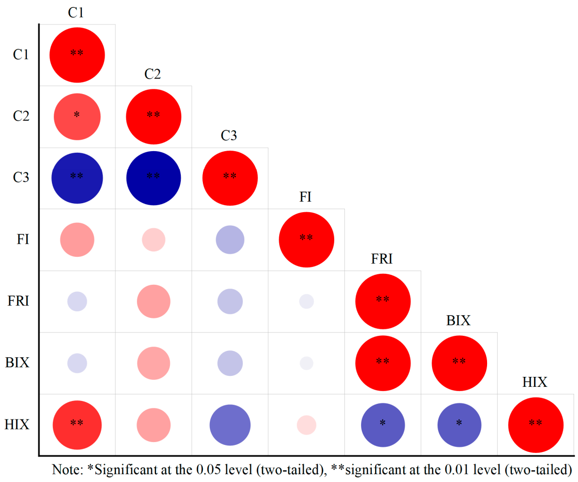

Figure 5. Correlation analysis between DOM fractions and fluorescence index in Yuanteng River.

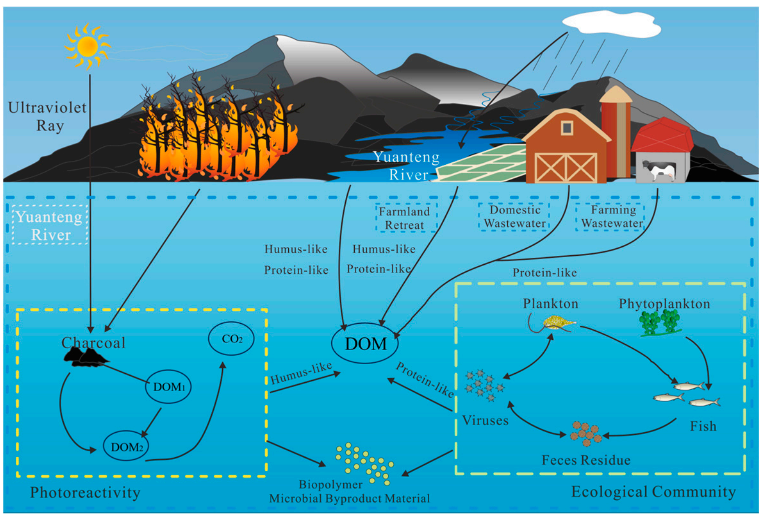

Figure 6. Schematic diagram of DOM sources in water bodies in the study area.

5. Conclusions

The fluorescence difference in dissolved organic matter in the water bodies of the Yuanteng River impacted by the hill fire exhibited significant characterization compared to normal water bodies. The fluorescence peaks of the UV humic-like A peak and the visible humic-like C peak were prominent in the dissolved organic matter of the Yuanteng River water body affected by the hill fire. However, the values of the B and T peaks were not as prominent compared to the DOM of the normal water body. This observation suggests that the hill fire resulted in an elevated content of humic-like substances in the Yuanteng River water body. The increased degree of vegetation humus post-burn may have led to higher-than-normal humus-like content in the water body of the Yuanteng River, while the burning during the hill fire could have depleted a significant amount of proteins, resulting in lower-than-normal protein-like content in the water body.

In the water column of the Yuanteng River impacted by the hill fire, three fluorescent fractions were observed: C1, resembling humic acid (fulvic acid); C2, comprising biopolymers, microbial by-products, and humic acid-like substances; and C3, consisting of proteins (tyrosine and tryptophan). The C1 and C2 components exhibit homology, with the red shift of the C1 peak possibly attributable to the elevated presence of aromatic compounds. The position of the C3 component is typical and can serve as a marker for tracing proteins. The microbial by-products and biopolymers DOM in the C2 fraction can be further analyzed for their composition and constitutive principles.

In the Yuanteng River water bodies impacted by the hill fire, the BIX, FRI, and HIX indices exhibited higher values compared to those in unaffected water bodies. Both humic acid-like and protein-like substances are influenced by a mixture of terrestrial and endogenous inputs. The impact of hill fires increases the content of terrestrial inputs of humus-like substances. In the water bodies of farmland areas in the Yuanteng River, dissolved organic matter formation and levels are closely linked to microbial activity, bacteria, and plankton in the water column. The correlation analysis reveals consistent variations in the source and composition of dissolved organic matter in the waters of the Yuanteng River.

Author Contributions: Writing—review and editing, conceptualization, K.S.; project administration, data analysis, and review, H.Z.; methodology and investigation, Z.R. All authors have read and agreed to the published version of the manuscript.

Funding: This work was funded by the Guangxi Key R&D Program (Guike-AB22080093, GuikeAB22035075, and Guike-AB21075007) and the Guilin Key R&D Program (20210212-2).

Data Availability Statement: The data presented in this study are available on request from the corresponding author.

Acknowledgments: The authors would like to sincerely thank the Guangxi Engineering Research Center of Comprehensive Treatment for Agricultural Non-point Source Pollution, and Modern Industry College of Ecology and Environmental Protection, Guilin University of Technology for their assistance.

Conflicts of Interest: The authors declare no conflicts of interest.

References

1. Dong, Y.; Li, Y.; Kong, F.; Zhang, J.; Xi, M. Source, Structural Characteristics and Ecological Indication of Dissolved Organic Matter Extracted from Sediments in the Primary Tributaries of the Dagu River. *Ecol. Indic.* **2020**, *109*, 105776. [CrossRef]
2. Benner, R.; Biddanda, B.; Black, B.; McCarthy, M. Abundance, Size Distribution, and Stable Carbon and Nitrogen Isotopic Compositions of Marine Organic Matter Isolated by Tangential-Flow Ultrafiltration. *Mar. Chem.* **1997**, *57*, 243–263. [CrossRef]
3. Keil, R.; Kirchman, D. Contribution of Dissolved Free Amino Acids and Ammonium to the Nitrogen Requirements of Heterotrophic Bacterioplankton. *Mar. Ecol. Prog. Ser.* **1991**, *73*, 1–10. [CrossRef]
4. Zhi, E.; Yu, H.; Duan, L.; Han, L.; Liu, L.; Song, Y. Characterization of the Composition of Water DOM in a Surface Flow Constructed Wetland Using Fluorescence Spectroscopy Coupled with Derivative and PARAFAC. *Environ. Earth Sci.* **2015**, *73*, 5153–5161. [CrossRef]
5. Sgroi, M.; Roccaro, P.; Korshin, G.V.; Greco, V.; Sciuto, S.; Anumol, T.; Snyder, S.A.; Vagliasindi, F.G.A. Use of Fluorescence EEM to Monitor the Removal of Emerging Contaminants in Full Scale Wastewater Treatment Plants. *J. Hazard. Mater.* **2017**, *323*, 367–376. [CrossRef] [PubMed]
6. Kowalczuk, P.; Cooper, W.J.; Durako, M.J.; Kahn, A.E.; Gonsior, M.; Young, H. Characterization of Dissolved Organic Matter Fluorescence in the South Atlantic Bight with Use of PARAFAC Model: Relationships between Fluorescence and Its Components, Absorption Coefficients and Organic Carbon Concentrations. *Mar. Chem.* **2010**, *118*, 22–36. [CrossRef]
7. Derrien, M.; Yang, L.; Hur, J. Lipid Biomarkers and Spectroscopic Indices for Identifying Organic Matter Sources in Aquatic Environments: A Review. *Water Res.* **2017**, *112*, 58–71. [CrossRef] [PubMed]

8. Kellerman, A.M.; Kothawala, D.N.; Dittmar, T.; Tranvik, L.J. Persistence of Dissolved Organic Matter in Lakes Related to Its Molecular Characteristics. *Nat. Geosci.* **2015**, *8*, 454–457. [CrossRef]
9. Wen, L.; Yang, F.; Li, X.; Liu, S.; Lin, Y.; Hu, E.; Gao, L.; Li, M. Composition of Dissolved Organic Matter (DOM) in Wastewater Treatment Plants Influent Affects the Efficiency of Carbon and Nitrogen Removal. *Sci. Total Environ.* **2023**, *857*, 159541. [CrossRef]
10. Shang, Y.; Wen, Z.; Song, K.; Liu, G.; Lai, F.; Lyu, L.; Li, S.; Tao, H.; Hou, J.; Fang, C.; et al. Natural versus Anthropogenic Controls on the Dissolved Organic Matter Chemistry in Lakes across China: Insights from Optical and Molecular Level Analyses. *Water Res.* **2022**, *221*, 118779. [CrossRef]
11. Kikuchi, T.; Fujii, M.; Terao, K.; Jiwei, R.; Lee, Y.P.; Yoshimura, C. Correlations between Aromaticity of Dissolved Organic Matter and Trace Metal Concentrations in Natural and Effluent Waters: A Case Study in the Sagami River Basin, Japan. *Sci. Total Environ.* **2017**, *576*, 36–45. [CrossRef]
12. Chen, H.; Lei, K.; Wang, X. Terrestrial Humic Substances in Daliao River and Its Estuary: Optical Signatures and Photoreactivity to UVA Light. *Environ. Sci. Pollut. Res.* **2016**, *23*, 6459–6471. [CrossRef]
13. Wang, X.; Wu, Y.; Bao, H.; Gan, S.; Zhang, J. Sources, Transport, and Transformation of Dissolved Organic Matter in a Large River System: Illustrated by the Changjiang River, China. *JGR Biogeosciences* **2019**, *124*, 3881–3901. [CrossRef]
14. Tshering, K.; Miotlinski, K.; Blake, D.; Boyce, M.C.; Bath, A.; Carvalho, A.; Horwitz, P. Effect of Fire on Characteristics of Dissolved Organic Matter in Forested Catchments in the Mediterranean Biome: A Review. *Water Res.* **2023**, *230*, 119490. [CrossRef] [PubMed]
15. Yamashita, Y.; Kojima, D.; Yoshida, N.; Shibata, H. Relationships between Dissolved Black Carbon and Dissolved Organic Matter in Streams. *Chemosphere* **2021**, *271*, 129824. [CrossRef]
16. Olefeldt, D.; Turetsky, M.R.; Blodau, C. Altered Composition and Microbial versus UV-Mediated Degradation of Dissolved Organic Matter in Boreal Soils Following Wildfire. *Ecosystems* **2013**, *16*, 1396–1412. [CrossRef]
17. Vergnoux, A.; Di Rocco, R.; Domeizel, M.; Guiliano, M.; Doumenq, P.; Théraulaz, F. Effects of Forest Fires on Water Extractable Organic Matter and Humic Substances from Mediterranean Soils: UV–Vis and Fluorescence Spectroscopy Approaches. *Geoderma* **2011**, *160*, 434–443. [CrossRef]
18. Dymov, A.A.; Startsev, V.V.; Milanovsky, E.Y.; Valdes-Korovkin, I.A.; Farkhodov, Y.R.; Yudina, A.V.; Donnerhack, O.; Guggenberger, G. Soils and Soil Organic Matter Transformations during the Two Years after a Low-Intensity Surface Fire (Subpolar Ural, Russia). *Geoderma* **2021**, *404*, 115278. [CrossRef]
19. Li, X.; Jin, H.; Wang, H.; Wu, X.; Huang, Y.; He, R.; Luo, D.; Jin, X. Distributive Features of Soil Carbon and Nutrients in Permafrost Regions Affected by Forest Fires in Northern Da Xing'anling (Hinggan) Mountains, NE China. *CATENA* **2020**, *185*, 104304. [CrossRef]
20. Bladon, K.D.; Silins, U.; Wagner, M.J.; Stone, M.; Emelko, M.B.; Mendoza, C.A.; Devito, K.J.; Boon, S. Wildfire Impacts on Nitrogen Concentration and Production from Headwater Streams in Southern Alberta's Rocky Mountains. *Can. J. For. Res.* **2008**, *38*, 2359–2371. [CrossRef]
21. Huguet, A.; Vacher, L.; Relexans, S.; Saubusse, S.; Froidefond, J.M.; Parlanti, E. Properties of Fluorescent Dissolved Organic Matter in the Gironde Estuary. *Org. Geochem.* **2009**, *40*, 706–719. [CrossRef]
22. Fellman, J.B.; Hood, E.; Spencer, R.G.M. Fluorescence Spectroscopy Opens New Windows into Dissolved Organic Matter Dynamics in Freshwater Ecosystems: A Review. *Limnol. Oceanogr.* **2010**, *55*, 2452–2462. [CrossRef]
23. Zhang, Y.; Zhang, E.; Yin, Y.; van Dijk, M.A.; Feng, L.; Shi, Z.; Liu, M.; Qin, B. Characteristics and Sources of Chromophoric Dissolved Organic Matter in Lakes of the Yungui Plateau, China, Differing in Trophic State and Altitude. *Limnol. Oceanogr.* **2010**, *55*, 2645–2659. [CrossRef]
24. Coble, P.G. Characterization of Marine and Terrestrial DOM in Seawater Using Excitation-Emission Matrix Spectroscopy. *Mar. Chem.* **1996**, *51*, 325–346. [CrossRef]
25. Coble, P.G.; Del Castillo, C.E.; Avril, B. Distribution and Optical Properties of CDOM in the Arabian Sea during the 1995 Southwest Monsoon. *Deep Sea Res. Part II Top. Stud. Oceanogr.* **1998**, *45*, 2195–2223. [CrossRef]
26. Stedmon, C.A.; Markager, S.; Bro, R. Tracing Dissolved Organic Matter in Aquatic Environments Using a New Approach to Fluorescence Spectroscopy. *Mar. Chem.* **2003**, *82*, 239–254. [CrossRef]
27. Zhang, Y.; Yin, Y.; Feng, L.; Zhu, G.; Shi, Z.; Liu, X.; Zhang, Y. Characterizing Chromophoric Dissolved Organic Matter in Lake Tianmuhu and Its Catchment Basin Using Excitation-Emission Matrix Fluorescence and Parallel Factor Analysis. *Water Res.* **2011**, *45*, 5110–5122. [CrossRef]
28. Moran, M.A.; Zepp, R.G. Role of Photoreactions in the Formation of Biologically Labile Compounds from Dissolved Organic Matter. *Limnol. Oceanogr.* **1997**, *42*, 1307–1316. [CrossRef]
29. Zhou, S.; Huang, C.; Han, B.; Xiao, Y.; Tang, J.; Xiang, Y.; Luo, C. Simulated Nitrogen Deposition Significantly Suppresses the Decomposition of Forest Litter in a Natural Evergreen Broad-Leaved Forest in the Rainy Area of Western China. *Plant Soil* **2017**, *420*, 135–145. [CrossRef]
30. Coble, P.G. Marine Optical Biogeochemistry: The Chemistry of Ocean Color. *Chem. Rev.* **2007**, *107*, 402–418. [CrossRef]
31. Seredynska-Sobecka, B.; Stedmon, C.A.; Boe-Hansen, R.; Waul, C.K.; Arvin, E. Monitoring Organic Loading to Swimming Pools by Fluorescence Excitation-Emission Matrix with Parallel Factor Analysis (PARAFAC). *Water Res.* **2011**, *45*, 2306–2314. [CrossRef] [PubMed]
32. Battin, T.J. Dissolved Organic Matter and Its Optical Properties in a Blackwater Tributary of the Upper Orinoco River, Venezuela. *Org. Geochem.* **1998**, *28*, 561–569. [CrossRef]

33. Stedmon, C.A.; Markager, S. Resolving the Variability in Dissolved Organic Matter Fluorescence in a Temperate Estuary and Its Catchment Using PARAFAC Analysis. *Limnol. Oceanogr.* **2005**, *50*, 686–697. [CrossRef]
34. He, W.; Hur, J. Conservative Behavior of Fluorescence EEM-PARAFAC Components in Resin Fractionation Processes and Its Applicability for Characterizing Dissolved Organic. *Water Res.* **2015**, *83*, 217–226. [CrossRef] [PubMed]
35. Bianco, A.; Minella, M.; De Laurentiis, E.; Maurino, V.; Minero, C.; Vione, D. Photochemical Generation of Photoactive Compounds with Fulvic-like and Humic-like Fluorescence in Aqueous Solution. *Chemosphere* **2014**, *111*, 529–536. [CrossRef] [PubMed]
36. Leenheer, J.A.; Croué, J.P. Characterizing Aquatic Dissolved Organic Matter. *Environ. Sci. Technol.* **2003**, *37*, 18A–26A. [CrossRef] [PubMed]
37. Xu, H.; Guo, L. Molecular Size-Dependent Abundance and Composition of Dissolved Organic Matter in River, Lake and Sea Waters. *Water Res.* **2017**, *117*, 115–126. [CrossRef] [PubMed]
38. Ziegelgruber, K.L.; Zeng, T.; Arnold, W.A.; Chin, Y.-P. Sources and Composition of Sediment Pore-Water Dissolved Organic Matter in Prairie Pothole Lakes. *Limnol. Oceanogr.* **2013**, *58*, 1136–1146. [CrossRef]
39. Ohno, T.; Fernandez, I.J.; Hiradate, S.; Sherman, J.F. Effects of Soil Acidification and Forest Type on Water Soluble Soil Organic Matter Properties. *Geoderma* **2007**, *140*, 176–187. [CrossRef]